

Efficient implementation of the non-Dyson third-order algebraic diagrammatic construction approximation for the electron propagator for closed- and open-shell molecules

Cite as: J. Chem. Phys. **150**, 064108 (2019); <https://doi.org/10.1063/1.5081674>

Submitted: 15 November 2018 . Accepted: 28 January 2019 . Published Online: 13 February 2019

Adrian L. Dempwolff , Matthias Schneider, Manuel Hodecker , and Andreas Dreuw 



View Online



Export Citation



CrossMark

ARTICLES YOU MAY BE INTERESTED IN

[Algebraic-diagrammatic construction scheme for the polarization propagator including ground-state coupled-cluster amplitudes. I. Excitation energies](#)

The Journal of Chemical Physics **150**, 174104 (2019); <https://doi.org/10.1063/1.5081663>

[Operators in quantum machine learning: Response properties in chemical space](#)

The Journal of Chemical Physics **150**, 064105 (2019); <https://doi.org/10.1063/1.5053562>

[Similarities and differences of the Lagrange formalism and the intermediate state representation in the treatment of molecular properties](#)

The Journal of Chemical Physics **150**, 164125 (2019); <https://doi.org/10.1063/1.5093606>

Lock-in Amplifiers
... and more, from DC to 600 MHz



Efficient implementation of the non-Dyson third-order algebraic diagrammatic construction approximation for the electron propagator for closed- and open-shell molecules

Cite as: J. Chem. Phys. 150, 064108 (2019); doi: 10.1063/1.5081674

Submitted: 15 November 2018 • Accepted: 28 January 2019 •

Published Online: 13 February 2019



View Online



Export Citation



CrossMark

Adrian L. Dempwolf,  Matthias Schneider, Manuel Hodecker,  and Andreas Dreuw^{a)} 

AFFILIATIONS

Interdisciplinary Center for Scientific Computing, Heidelberg University, Im Neuenheimer Feld 205, D-69120 Heidelberg, Germany

^{a)}Electronic mail: dreuw@uni-heidelberg.de

ABSTRACT

A novel efficient implementation of the non-Dyson algebraic diagrammatic construction (ADC) scheme of the $(N - 1)$ -part of the electron propagator up to third order of perturbation theory is presented. Due to the underlying spin-orbital formulation, for the first time, the computation of ionization potentials of open-shell radicals is thus possible via non-Dyson ADC schemes. Thorough evaluation of the accuracy, applicability, and capabilities of the new method reveals a mean error of 0.15 eV for closed- as well as open-shell atoms and molecules.

Published under license by AIP Publishing. <https://doi.org/10.1063/1.5081674>

I. INTRODUCTION

The ionization potential (IP) is a fundamental molecular property defined as the energy required to remove one electron from the system, thus corresponding to the energy difference between the final ionized state and the initial neutral state. From this perspective, IPs are one-electron properties and can often be interpreted with reasonable accuracy in the single-particle picture of molecular orbitals (MOs) and their corresponding orbital energies. However, the single-particle picture breaks down for higher ionization potentials as well as in strongly correlated systems.¹

Ionization potentials are physical observables that can be measured in the gas phase, for example, via photoelectron or photoemission (PE) spectroscopy.² In these experiments, the molecules are ionized by X-ray or the UV radiation of the photon energy E_{ph} and the kinetic energy E_{kin} of the emitted electron is recorded, yielding the photoelectron spectrum. The spectrum is directly related to ionization potentials via the equation $\text{IP} = E_{\text{ph}} - E_{\text{kin}}$, reflecting Einstein's

explanation of the photoelectric effect.² More recently, time-resolved PE spectroscopy was used successfully to investigate reaction intermediates.^{3,4} Furthermore, the IP is also of general interest to chemical and material science since it is directly related to oxidation potentials and can thus serve as a molecular “ruler” for hole transport materials in organic semi-conductors.^{5,6}

The simplest and most straightforward way for a theoretical estimation of IPs is to rely on theorems of Koopman or Janak in Hartree-Fock (HF) or density functional theory (DFT), respectively, which are valid in the single-particle picture and state that the negative energy of an occupied orbital is equal to the ionization potential.^{7,8} Koopmans' theorem (KT) is usually a fairly accurate first approximation since two effects are neglected, i.e., orbital relaxation upon ionization and electron correlation (in the HF case), which counteract one another. The typical error, however, is still of the order of 1–2 eV.

A possible way to improve upon Koopmans' theorem is to perform two separate self-consistent field (SCF) HF

calculations for the neutral N -electron and the ionized $(N - 1)$ -electron species and to take the difference of the two absolute energies. This approach is referred to as Δ SCF method which, however, usually underestimates IPs since the cationic species is stabilized due to the inclusion of orbital relaxation, while electron correlation is still neglected. The latter can be accounted for by using, e.g., second-order Møller-Plesset (MP) perturbation theory or coupled-cluster methods,^{9,10} yielding so-called Δ MP2 or Δ CC values. Furthermore, all of these “ Δ -methods” suffer from the disadvantages that two separate calculations have to be carried out, which do not necessarily converge to the desired state, and that the intrinsic errors of the two calculations accumulate.

Thus, it is generally desirable to obtain IPs directly in one calculation. To this end, several quantum chemical methods have been developed. In particular, various Green's function or propagator^{11,12} based computational schemes,^{1,13-21} including the so-called outer-valence Green's function (OVGF) method, are available.²¹⁻²³ Other high-level methods include the equation-of-motion (EOM) coupled cluster (CC)²⁴⁻²⁷ based approaches for the treatment of ionization, termed EOM-IP-CC.²⁸⁻³¹ Another closely related propagator method is the algebraic diagrammatic construction (ADC) scheme of the one-particle Green's function,^{19-21,32} which is considered in this paper.

Here, an efficient implementation of the non-Dyson (nD) ADC(3) scheme for the electron propagator³³⁻³⁵ in a spin-orbital formulation is reported, allowing for the first time for the calculation of open-shell molecular systems. ADC schemes are in general Hermitian and represent an optimal combination of accuracy and computational efficiency, which is known as the compactness property.^{33,36,37} Furthermore, ADC is size consistent,³⁸ thus guaranteeing size-intensive results for transition energies and amplitudes.

In Sec. II, the basic theoretical concepts of ADC are outlined, followed by a brief overview of the implementation. Afterwards, the accuracy and applicability of the implemented methods are evaluated in a number of selected closed- and open-shell test applications. A summary and conclusions are given in Sec. VI.

II. THEORY

The working equations of the IP-ADC approximation scheme for the electron propagator^{33,34} were originally derived via the one-particle Green's function.¹⁹⁻²¹ However, an alternative route for its derivation exists via the so-called *intermediate state representation* (ISR) formalism.^{36,37,39} This route is based on correlated $(N - 1)$ -electron states which are obtained by acting with an ionization operator \hat{C}_J on the formally exact N -electron ground state $|\Psi_0^N\rangle$,

$$|\Psi_J^0\rangle = \hat{C}_J |\Psi_0^N\rangle. \quad (1)$$

Here, the ionization operator \hat{C}_J consists of creation and annihilation operators $\hat{c}_{p\sigma}^\dagger$ and $\hat{c}_{q\tau}$ of second quantization that create one-hole (1h), two-hole-one-particle (2h-1p), ..., configurations with respect to the HF reference

state,

$$\{\hat{C}_J\} = \{\hat{c}_{i\sigma}, \hat{c}_{a\sigma}^\dagger \hat{c}_{i\sigma} \hat{c}_{j\tau}, \hat{c}_{b\sigma}^\dagger \hat{c}_{a\tau}^\dagger \hat{c}_{i\sigma} \hat{c}_{j\tau} \hat{c}_{k\nu}, \dots\}; \quad (2)$$

$$a < b < \dots, i < j < k < \dots,$$

where the subscripts a, b, \dots and i, j, \dots label unoccupied (virtual) and occupied orbitals in the HF determinant, and the subscripts p, q, \dots stand for either occupied or unoccupied orbitals. In addition, for unrestricted ADC, electron spin has to be taken into account, indicated by the spin labels σ, τ, \dots . Thus, the annihilation and creation operators act on spin rather than spatial orbitals, and care has to be taken to assure that the desired eigenfunctions of the spin operator are generated. In a subsequent specific orthonormalization procedure, the correlated ionized states $|\Psi_J^0\rangle$ are transformed to the basis of so-called intermediate states (IS) $\{|\tilde{\Psi}_J^{N-1}\rangle\}$.

Representing the Hamiltonian, shifted by the energy of the N -electron ground state, within the orthonormal basis of ionized intermediate states

$$M_{IJ} = \langle \tilde{\Psi}_I^{N-1} | \hat{H} - E_0^N | \tilde{\Psi}_J^{N-1} \rangle, \quad (3)$$

results in a Hermitian eigenvalue equation of the form

$$\mathbf{M}\mathbf{Y} = \mathbf{Y}\mathbf{\Omega}, \quad \mathbf{Y}^\dagger \mathbf{Y} = \mathbf{1}, \quad (4)$$

where \mathbf{Y} is the matrix of eigenvectors Y_n and $\mathbf{\Omega}$ is the diagonal matrix of eigenvalues

$$\Omega_n = E_n^{N-1} - E_0^N, \quad (5)$$

which correspond to the ionization potentials. The exact ionized states $|\Psi_n^{N-1}\rangle$ can then be expressed in terms of the intermediate states as

$$|\Psi_n^{N-1}\rangle = \sum_J Y_{Jn} |\tilde{\Psi}_J^{N-1}\rangle. \quad (6)$$

The elements of the ADC eigenvectors $Y_{Jn} = \langle \tilde{\Psi}_J^{N-1} | \Psi_n^{N-1} \rangle$ are thus the expansion coefficients of the exact ionized states in the IS basis. However, since neither the exact ground state $|\Psi_0^N\rangle$ nor its energy E_0^N are known, both are expanded according to the MP perturbation series and thus also the ADC matrix itself is expanded,

$$\mathbf{M} = \mathbf{M}^{(0)} + \mathbf{M}^{(1)} + \mathbf{M}^{(2)} + \dots \quad (7)$$

Taking the n th order MP ground state (MP n) as reference, the corresponding IP-ADC(n) approximation is obtained, yielding results for ionization energies of primary hole states correct up to n th order of perturbation theory.

In addition, spectral amplitudes are available through the relation

$$\mathbf{x} = \mathbf{Y}^\dagger \mathbf{f}, \quad (8)$$

where \mathbf{f} are the effective transition moments according to

$$f_{Ip} = \langle \tilde{\Psi}_I^{N-1} | \hat{c}_p | \Psi_0^N \rangle, \quad (9)$$

which are expanded in a perturbation series similar to \mathbf{M} . The relative spectral intensities P_n are accessible as pole strengths, which can be calculated from the spectral amplitudes as

$$P_n = \sum_p |x_{np}|^2. \quad (10)$$

Explicit expressions for the IP-ADC matrix and effective transition moment elements up to third order can be found in the literature.³⁵

Apart from an alternative derivation route to IP-ADC, the ISR also gives direct access to other properties which had not been available before in the electron propagator approach. For example, the expectation value of any one-particle operator \hat{O} of the ionized ADC states

$$O_{mn} = \langle \Psi_m^{N-1} | \hat{O} | \Psi_n^{N-1} \rangle \quad (11)$$

can be represented in the basis of IS states by using Eq. (6) as

$$O_{mn} = \sum_{IJ} Y_{mI} \langle \tilde{\Psi}_I^{N-1} | \hat{O} | \tilde{\Psi}_J^{N-1} \rangle Y_{Jn} = Y_m^\dagger \tilde{\mathbf{O}} Y_n, \quad (12)$$

where $\tilde{\mathbf{O}}$ is the matrix representation of the operator \hat{O} in the IS basis, $\tilde{O}_{IJ} = \langle \tilde{\Psi}_I^{N-1} | \hat{O} | \tilde{\Psi}_J^{N-1} \rangle$. In other words, once the one-particle operator is represented in the known IS basis, it just needs to be contracted with the corresponding ADC vector to obtain the expectation value of the corresponding ionized ADC state.

III. IMPLEMENTATION

Restricted and unrestricted IP-ADC up to third order have been implemented in `adcmn`,⁴⁰ a suite of ADC methods for electronically excited and ionized states, which currently is available as part of the quantum chemical program package Q-CHEM.⁴¹ The implementation makes use of the tensor library `libtensor`,⁴² which features parallelization of tensor algebra operations in a shared memory environment as well as handling of spin, point group, and permutational symmetry. Apart from closed-shell systems, the presented implementation can also handle open-shell systems. The eigenvalue problem Eq. (4) is solved using matrix-free methods, i.e., the Davidson algorithm,⁴³ yielding the lowest-lying ionized states by iterative refinement of vectors by means of computing matrix vector products **MY**. The corresponding pole strengths of the ionization processes are computed at second order of perturbation theory for both the IP-ADC(2) and IP-ADC(3) schemes, giving direct access to photoelectron spectra.

With O and V denoting the number of occupied and virtual orbitals, respectively, the formal scaling of the presented implementation is O^3V^2 for IP-ADC(2), which results from the iteratively evaluated matrix vector products. In the case of IP-ADC(3), two implementations have been considered. One involves the iterative computation of matrix vector products scaling with OV^4 . However, by precomputing the $1h-1h$ block equation (A8) of the IP-ADC(3) matrix in a single step formally scaling with O^2V^4 , the scaling of the iteratively evaluated part is reduced to O^3V^2 , thereby leading to a reasonable overall performance enhancement in virtually all practical cases. The implemented equations are given in the Appendix. Therein, the index restrictions appearing in the original IP-ADC matrix equations have been lifted for the sake of efficient evaluation in the framework of the `libtensor` library. This is achieved by demanding anti-symmetry of the $2h-1p$ part of the state

vectors Y_n with respect to the permutation of the two occupied indices and additionally introducing appropriate scaling factors in order to account for double counting.

IV. COMPUTATIONAL DETAILS

All calculations discussed in this work were carried out using the Q-CHEM 5.0.2 or 5.1 software.⁴¹ The ground state geometries of all shown molecules were optimized with restricted or unrestricted variants of the Møller-Plesset perturbation theory of second order (MP2)⁹ employing the cc-pVTZ basis set.⁴⁴⁻⁴⁶ In the case of the amino acids, a single conformation was selected following Ref. 47. The resulting structures were characterized as equilibrium geometries in subsequent frequency calculations. An exception is the galvinoxyl free radical, where we directly used the geometry available through the supplementary material of Ref. 48.

Unless stated otherwise, the cc-pVTZ basis set was employed in the IP-ADC calculations. All simulated spectra were simulated with Lorentzian line-shapes on the calculated IPs, using the computed pole strengths as intensities and a full width at half maximum (fwhm) of 0.5 and 0.6 eV for the galvinoxyl free radical and glycine, respectively. Where an assignment was made between computed ionization potentials and experimental data, this was performed based on careful consideration of the shape of the respective spectra. Only ionization potentials having a zeroth order pole strength of $P > 0.85$ were taken into account.

V. RESULTS AND DISCUSSION

In order to demonstrate the capabilities of the novel implementation and to study the performance and the accuracy, in particular, of unrestricted IP-UADC, ionization potentials of a variety of closed- and open-shell systems have been computed employing different IP-(U)ADC schemes and compared to experimental data.

A. Closed-shell molecules: Amino acids

Restricted IP-ADC up to third order has been applied for the calculation of the five to seven lowest vertical ionization potentials of the amino acids such as glycine, alanine, serine, tyrosine, and methionine shown in Fig. 1. The computed IPs are summarized in Table I and compared to the experimental data taken from Ref. 49.

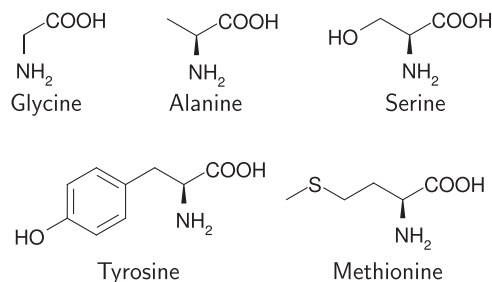


FIG. 1. Molecular structures of selected amino acids.

TABLE I. Computed values for the lowest vertical ionization energies of selected amino acids compared to experimental data. All values are given in eV.

System	State	Expt. ^a	IP-ADC(3)	IP-ADC(2)	Δ MP2	Δ B3LYP
Glycine	1	10.0	10.11	9.44	10.25	9.80
	2	11.1	11.37	9.95		
	3	12.2	12.28	11.46		
	4	13.6	13.57	13.19		
	5	14.4	14.70	13.50		
Alanine	1	9.85	9.95	9.24	10.11	9.61
	2	11.0	11.16	9.77		
	3	12.1	12.14	11.31		
	4	12.8	12.85	12.40		
	5	13.4	13.50	12.90		
Serine	1	10.0	10.28	9.39	10.60	9.66
	2	11.0	10.99	10.00		
	3	11.25	11.44	10.09		
	4	12.0				
	5	12.4	12.24	11.41		
	6	12.6	12.77	11.81		
Tyrosine	1	8.5	8.34	8.10	9.10	8.26
	2	9.4	9.29	8.78		
	3	9.6	9.97	9.20		
	4	10.8	11.08	10.13		
	5	11.3	11.31	10.43		
Methionine	1	8.65	8.79	8.50	8.86	8.48
	2	9.8	10.08	8.94		
	3	10.9	11.30	10.41		
	4		11.37	10.67		
	5		11.50	11.04		
	6	12.1	12.23	11.52		
	7	12.6	12.91	12.45		
$ \Delta_{\max} $			0.40	1.23	0.60	0.34
$\Delta_{\text{abs}}; \Delta$			0.17; 0.13	0.68; -0.68	0.38; 0.38	0.24; -0.24
$\sigma(\Delta)$			0.16	0.29	0.20	0.06

^aExperimental data from Ref. 49. The stated values refer to band maxima.

Inspecting first the values of the IPs obtained at the IP-ADC(2) level, for this selected set of ionized states, the mean absolute error (MAE) with respect to the experimental results is 0.68 eV. The mean signed error (MSE) of -0.68 eV indicates the IPs to be systematically underestimated at this level of theory, resulting in quite accurate relative energies of the ionized states, where the width of the error distribution is found to be 0.29 eV. The corresponding photoelectron spectra are thus shifted by an energy shift of about 0.7 eV to lower energies. The IPs computed at the IP-ADC(3) level exhibit a considerably smaller mean absolute error of only 0.17 eV and a mean signed error of 0.13 eV along with a smaller standard deviation of the error of 0.16 eV, showing a more balanced and slightly less scattered error distribution than in the case of IP-ADC(2). This agrees with the results obtained by Trofimov and Schirmer, who obtained a mean error of the IPs of C₂H₄, CO, CS, F₂, H₂CO, H₂O, HF, N₂, and Ne of about 0.2 eV relative to the experimental values and full configuration interaction (FCI) results.³⁴

For comparison, the first ionization potentials have also been calculated using Δ MP2 and Δ B3LYP. With these methods, only the lowest IP is directly accessible as the energy difference of the electronic ground states of the cation and the neutral species. For higher IPs, the ground state DFT/B3LYP or MP2 calculation of the cation needs to be tweaked to converge to a higher lying electronic state by some constraint. Inspecting Table I, MP2 can be recognized to consistently overestimate the corresponding values with a mean (absolute) error of 0.38 eV and an error spread of 0.20 eV, while the opposite is the case for DFT/B3LYP, for which a smaller mean absolute error of 0.24 eV together with a mean signed error of -0.24 eV is found. For the lowest IPs of the amino acids, Δ B3LYP yields rather consistently shifted values, reflected in a small standard deviation of the error of only 0.06 eV. However, for the computation of higher IPs or the simulation of photoelectron spectra, Δ -methods are not applicable due to the above mentioned technical difficulties.

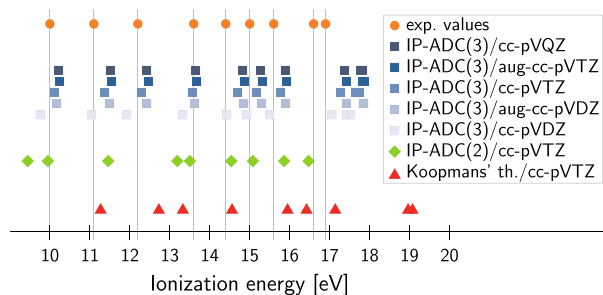
TABLE II. Vertical ionization energies of glycine computed using different basis sets and employing different IP-ADC schemes. All stated values are given in eV.

State	Expt. ^a	IP-ADC(3)					IP-ADC(2)	KT
		cc-pVQZ	aug-cc-pVTZ	cc-pVTZ	aug-cc-pVDZ	cc-pVDZ	cc-pVTZ	cc-pVTZ
1	10.0	10.22	10.25	10.11	10.17	9.76	9.44	11.27
2	11.1	11.51	11.55	11.37	11.49	11.04	9.95	12.73
3	12.2	12.43	12.47	12.28	12.42	11.93	11.46	13.33
4	13.6	13.66	13.68	13.57	13.62	13.32	13.19	14.56
5	14.4	14.83	14.86	14.70	14.85	14.42	13.50	15.95
6	15.0	15.27	15.31	15.17	15.31	14.93	14.54	16.42
7	15.6	15.89	15.93	15.77	15.91	15.51	15.08	17.14
8	16.6	17.38	17.42	17.28	17.42	17.05	15.86	18.96
9	16.9	17.78; 17.83	17.83; 17.86	17.66; 17.75	17.85; 17.85	17.42; 17.53	16.48	19.08
$ \Delta_{\max} $		0.91	0.95	0.81	0.95	0.58	1.15	2.36
$\Delta_{\text{abs}}; \Delta$		0.40; 0.40	0.43; 0.43	0.29; 0.28	0.36; 0.36	0.23; 0.00	0.66; -0.66	1.56; 1.56
$\sigma(\Delta)$		0.28	0.28	0.28	0.26	0.31	0.25	0.46

^aExperimental data from Ref. 49. The stated values refer to band maxima.

In order to study the basis set dependence of the IPs computed with IP-ADC(3), we calculated the lowest ionization potentials of glycine with a number of different basis sets. The results are compared to IP-ADC(0), which is equivalent to Koopmans' theorem, and IP-ADC(2), summarized in Table II and visualized in Fig. 2. Koopmans' theorem and IP-ADC(2) are noticed to perform overall quite poorly with errors of 1.56 ± 0.46 and -0.66 ± 0.25 eV, respectively. Regarding IP-ADC(3), the largest change in the spectrum is observed when augmenting the cc-pVDZ double-zeta basis set. Indeed, the ionization spectrum is consistently shifted to higher energies by approximately 0.4 eV, thereby preserving the spectral shape. This can readily be rationalized because an ionized, cationic species benefits less from the inclusion of diffuse basis functions than the neutral system does due to its more compact electronic structure. Further increasing the number of basis functions does not significantly improve the spectrum. The difference between the aug-cc-pVDZ and cc-pVQZ results, for example, is found to be below 0.1 eV for each calculated state. For all basis sets evaluated in the IP-ADC(3) computations, the standard deviation of the error is found to be in the range of 0.3 eV.

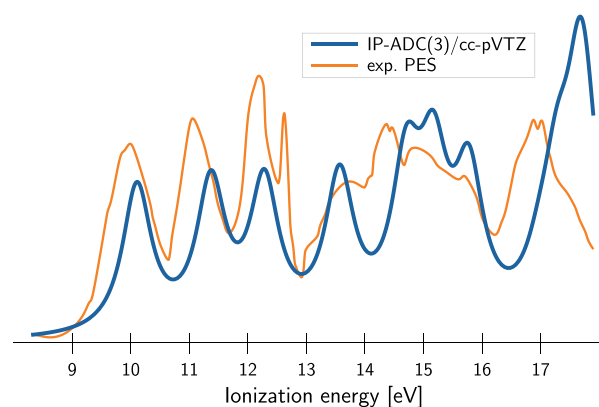
Inspecting Fig. 2, IP-ADC(2) becomes apparent not to possess sufficient accuracy to be useful for a reliable assignment

**FIG. 2.** Vertical ionization energies of glycine computed with different IP-ADC schemes and compared to the experimental data from Ref. 49.

of lines in experimental photoelectron spectra. A third-order calculation, by contrast, correctly reproduces the shape of the experimental spectrum even with small basis sets. This is also demonstrated by Fig. 3, where the recorded photoelectron spectrum of glycine as taken from Ref. 49 is compared to the corresponding simulated spectrum obtained at the IP-ADC(3)/cc-pVTZ level of theory. Despite the fact that only electronic contributions are considered in the simulated spectrum and vibrational effects are ignored, it reproduces the key features of the experimental spectrum remarkably well.

B. Open-shell atoms and molecules

With our novel implementation of IP-ADC, also an unrestricted version of IP-ADC, labeled IP-UADC, has become available for the first time, providing a convenient way for the computation of ionization potentials of open-shell systems. To evaluate the accuracy of IP-UADC, the ionization potentials of a variety of different open-shell systems have been computed

**FIG. 3.** Calculated photoelectron spectrum of glycine (blue). For comparison, the experimental spectrum as taken from Ref. 49 (orange) is shown.

and compared to available experimental data. The tested systems range from selected IPs of atoms and smaller radicals to the simulation of the photoelectron spectrum of the large organic galvinoxyl free radical.

1. Atoms

As a first fundamental test, the ionization potentials of the first- to third-row atoms have been calculated using IP-UADC up to third order. Although it is known that unrestricted HF (UHF) is unable to correctly describe the N -electron ground state of atoms with open-shell p^n configuration,³² we consider this a viable test to see whether IP-UADC is capable of reproducing the well-known trends of the IPs of the elements. The computed values of the IPs at KT (IP-UADC(0)), IP-UADC(2), and IP-UADC(3) level are listed in Table III and compared to the experimental gas phase values.

Having first a brief look at the IPs obtained at the level of KT, they reveal a mean absolute error of 0.46 eV and a mean signed error of 0.23 eV, with the standard deviation of the error being as large as 0.59 eV. In view of the drastic underlying approximations and the fact that KT is only conditionally applicable in the case of UHF,⁵¹ the error is surprisingly small and the computed IPs reproduce the trend of the IPs among the elements already at this rather low level of theory. However, the error is certainly too large to study IPs quantitatively. Going to IP-UADC(2), the error in the IPs is reduced with a mean absolute error of 0.34 eV and a mean signed error of -0.32 eV. As in the closed-shell case discussed above, IP-UADC(2) predominantly underestimates the first ionization potential. The largest single deviation is found for neon with 1.47 eV. Compared to KT, the improvement of the accuracy of the computed IPs is only moderate; however, a more

TABLE III. Experimental and computed values at IP-UADC(3), IP-UADC(2), and Koopmans' theorem level for the lowest ionization potential of first to third-row atoms. All values are given in eV.

Atom	Expt. ^a	IP-UADC(3)	IP-UADC(2)	KT
He	24.59	24.47	24.54	24.97
Li	5.39	5.35	5.35	5.34
Be	9.32	9.04	8.90	8.42
B	8.30	8.18	8.40	8.65
C	11.26	11.13	11.30	11.91
N	14.53	14.43	14.43	15.47
O	13.62	13.37	12.92	14.15
F	17.42	17.36	16.35	18.40
Ne	21.56	21.74	20.09	23.00
Na	5.14	5.00	4.98	4.96
Mg	7.65	7.45	7.35	6.89
Al	5.99	5.87	5.90	5.93
Si	8.15	8.04	8.10	8.18
P	10.49	10.41	10.49	10.65
S	10.36	10.04	10.00	10.29
Cl	12.97	12.69	12.57	13.05
Ar	15.76	15.57	15.38	16.06
$ \Delta_{\max} $		0.32	1.47	1.44
$\Delta_{\text{abs}}; \Delta$		0.16; -0.14	0.34; -0.32	0.46; 0.23
$\sigma(\Delta)$		0.11	0.42	0.59

^aExperimental data from NIST ASD.⁵⁰

consistent behavior is found, with the width of the error distribution being 0.42 eV. A major improvement of the accuracy of IPs is achieved when going to IP-UADC(3). The mean absolute error is reduced to as little as 0.16 eV, and a mean signed error of -0.14 eV is observed. At this level, also the largest single deviation is as small as 0.32 eV for sulfur, and the small standard deviation of the error of 0.11 eV makes IP-UADC(3) a reliable benchmark method across the first three rows of the periodic table. The first ionization potentials of first- to third-row atoms as calculated with IP-UADC(3) and Koopmans' theorem are visualized in Fig. 4, again emphasizing the overall good performance of IP-UADC(3). Summarizing the results of this first test, the accuracy of the IP-UADC methods increases in the expected order of $\text{KT} < \text{IP-UADC}(2) < \text{IP-UADC}(3)$. In addition, the unrestricted IP-ADC schemes possess the same overall accuracy as the restricted ones.

2. Small radicals

Going beyond atoms, the accuracy of IP-UADC was further studied by calculating the first ionization potential of the five small radicals such as hydroxyl, silyl, methyl, ethyl, and benzyl, for which experimental gas phase values are available for comparison.⁵²⁻⁵⁶ The computed IPs at the levels of KT, IP-UADC(2), as well as IP-UADC(3) are compiled in Table IV.

Inspecting first the computed IPs at the level of Koopmans' theorem, they exhibit a mean absolute and signed error of 0.78 eV, with the standard deviation of the error being 0.23 eV. The largest single error is 0.98 eV for the ethyl radical. Although the trend of the first IPs among the investigated radical species is reasonably well reproduced, KT is not useful as a quantitative method to predict the IPs reliably. At the IP-UADC(2) level, the corresponding errors are 0.30 and -0.24 eV, and the largest single deviation with respect to experimental results is found to be 0.91 eV for the hydroxyl radical, which is nearly as large as the maximum error of KT. The width of the error distribution is found to be 0.40 eV, thereby being even larger than in the case of KT. A quantitative agreement of the computed IPs and the experimental values is only achieved at

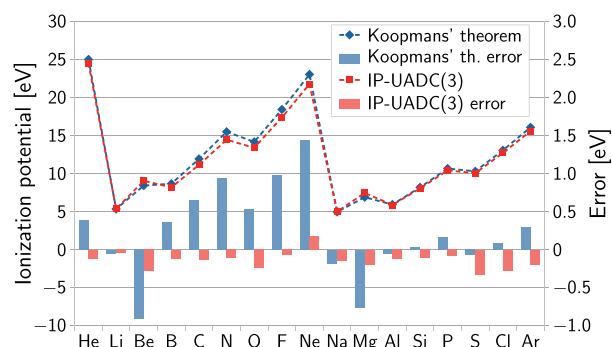


FIG. 4. First ionization potential of first, second, and third row atoms calculated with IP-UADC(3) (blue) and by means of Koopmans' theorem (red) employing the cc-pVTZ basis set along with the corresponding error with respect to experimental data.⁵⁰

TABLE IV. Experimental and computed values for the lowest vertical ionization potential of the radicals such as hydroxyl, silyl, methyl, ethyl, and benzyl at the theoretical level of KT and IP-UADC of second and third orders. All values are given in eV.

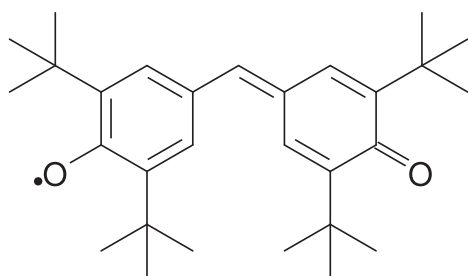
Radical	Expt.	IP-UADC(3)	IP-UADC(2)	KT
Hydroxyl ^a	13.02	12.98	12.11	13.88
Silyl ^b	8.74	8.79	8.87	9.19
Methyl ^c	9.84	9.71	9.60	10.46
Ethyl ^d	8.51	8.57	8.40	9.49
Benzyl ^e	7.43	7.37	7.34	8.40
$ \Delta_{\max} $		0.13	0.91	0.98
$\Delta_{\text{abs}}; \Delta$		0.07; -0.02	0.30; -0.24	0.78; 0.78
$\sigma(\Delta)$		0.08	0.40	0.23

^aExperimental value from Ref. 52.^bExperimental value from Ref. 53.^cExperimental value from Ref. 54.^dExperimental value from Ref. 55.^eExperimental value from Ref. 56.

the IP-UADC(3) level showing a very small MAE and MSE of only 0.07 and -0.02 eV, respectively, with the standard deviation of the error being 0.08 eV and the largest absolute error being 0.13 eV for the methyl radical. For these radicals, the IP-UADC(3) results are even more accurate than for the atoms. Since ADC methods are based on an MP ground state, this is not too surprising because—in contrast to the p^n open-shell atoms—doublet ground states as found in the considered radicals are usually well described by UHF and the subsequent MP treatment.

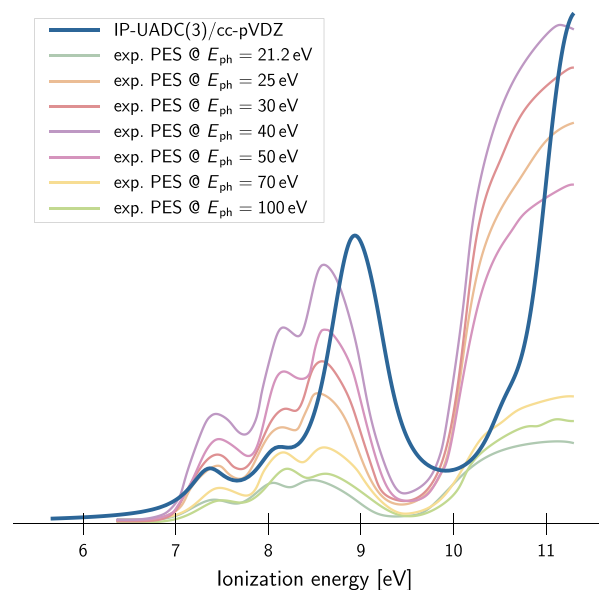
3. Galvinoxyl free radical

Finally, the photoelectron spectrum of the galvinoxyl free radical $C_{29}H_{41}O_2$ (Fig. 5) has been simulated using IP-UADC(3) to demonstrate the large-scale capability of our implementation and to further test the approach for larger organic molecules. It is a stable radical and serves as a radical scavenger and as a mechanistic probe for radical chain processes.⁵⁷ It is also used in synthesis as an inhibitor of undesired competitive radical reactions.^{58,59} The IP-UADC(3) calculation of its ionization spectrum employed the cc-pVDZ basis set, resulting in 639 basis functions. For this system size, an IP-UADC(3) calculation can still be performed with reasonable computational effort, i.e., the calculation can be performed on a 20-core machine within less than two days

**FIG. 5.** Molecular structure of the galvinoxyl free radical.

if sufficient memory is available. Altogether, the lowest 40 ionized states and corresponding IPs have been computed, and the spectrum has been simulated by convolution of the stick spectrum with a Lorentzian line-shape function of 0.6 eV fwhm. The computed spectrum has not been shifted in energy for the comparison with the experimental ones, and it is depicted in Fig. 6 together with experimental data recorded at different photon energies.⁴⁸

All peaks visible in the recorded experimental spectra are reproduced by the simulated spectrum at the IP-UADC(3) level. In particular, the energetically lower-lying ionization potentials are well reproduced, and also the intensity pattern is reasonable, although at the experimental side it depends on the photon energy used for ionization. For higher ionization potentials, however, larger deviations of the peak positions are observed. This may have different reasons. Especially for energetically higher ionization potentials, the measured IP may substantially differ from a calculated value assuming vertical ionization mechanism since vibrational contributions become more important favoring adiabatic electron loss. Hence, a shift toward lower IPs is seen in the experimental spectrum. At high photon energies and high IPs, one may also reach the double ionization threshold; that is, the singly ionized states are embedded in the electronic continuum, and basis set as well as many-body effects come into play which are not contained in the current, straightforwardly applied IP-UADC(3) methodology. However, given the simplicity of the single IP-UADC(3) black-box calculation and the naive construction of the spectrum using a Lorentzian convolution, the overall agreement between the simulated spectrum and the experimental one is remarkably good.

**FIG. 6.** Photoelectron spectrum of the galvinoxyl free radical. The spectrum simulated with IP-UADC(3) employing the cc-pVDZ basis set (blue) is compared to the experimental results taken from Ref. 48.

VI. SUMMARY AND CONCLUSIONS

The implementation of an efficient program of the non-Dyson algebraic diagrammatic construction scheme for the electron propagator, denoted IP-ADC, up to third order into the adcmn module of the Q-CHEM program package has been reported. The implementation features a restricted and, for the first time, an unrestricted IP-ADC version, which allows for the calculation of ionization potentials and ionization spectra of open-shell molecules based on an unrestricted Hartree-Fock reference. To demonstrate the accuracy, capabilities, and applicability of the method, we have tested it on selected closed- and open-shell atoms and molecules. For closed-shell IP-ADC, we have chosen amino acids as representative examples for organic molecules due to the large variety of functional groups present. The IP-UADC methods were tested for all atoms of the first, second, and third rows of the periodic table, small representative radicals, as well as the galvinoxyl radical. The accuracy of the tested restricted and unrestricted IP-ADC(n) approaches is similar. While Koopmans' theorem delivers only qualitative trends correctly and has the well-known error of about 0.5–1 eV, the mean error of IP-ADC(2) is reduced to about 0.3 eV, but outliers with significantly larger errors are still found. IP-ADC(3) is found as the first method of this family to provide accurate IPs with a mean error of less than 0.15 eV, even when moderate basis sets of cc-pVTZ or cc-pVDZ quality are used, allowing for the calculation of larger molecules.

A single IP-ADC(3) calculation does not only deliver the lowest IP of a molecular system but also yields the full ionization spectrum, which conveniently allows for the simulation of photoelectron spectra. Using the galvinoxyl radical as an representative example, its photoelectron spectrum has been computed at the IP-UADC(3) level and compared with experimental spectra. All major features of the low-energy regime are reproduced with high accuracy, although vibrational and temperature effects are modelled only implicitly by convoluting the electronic contributions to the spectrum with Lorentzian functions. Thereby, the restricted and unrestricted versions of IP-ADC(3) have proven to serve as useful tools for the assignment of experimentally observed IPs, the simulation of photoelectron spectra, and the description of ionization-related processes in molecular systems. In the future, various functionalities will be added to the IP-ADC program to allow for analysis of the ionized states and for inclusion of environment models. In addition, the potential of IP-ADC(3) for the investigation of properties of open-shell molecules based on a closed-shell reference state, in analogy to the well-known EOM-IP-CC approaches, shall be exploited.

SUPPLEMENTARY MATERIAL

See [supplementary material](#) for geometries of all considered molecules and a listing of the IPs computed for the galvinoxyl radical.

ACKNOWLEDGMENTS

A.L.D., M.S., and M.H. acknowledge financial support from the Heidelberg Graduate School “Mathematical and

Computational Methods for the Sciences” (GSC 220) funded by the German Research Foundation. Furthermore, A.L.D. acknowledges financial support from the Research Unit “Intermolecular and Interatomic Coulombic Decay” (FOR 1789) funded by the German Research Foundation.

APPENDIX: IMPLEMENTED EQUATIONS

In the following, we collect the IP-ADC matrix vector product equations and the expressions for the second-order pole strength as implemented in adcmn. The implementation follows the IP-ADC matrix equations given in Ref. 33. Parts of the equations have been optimized under the assumption that real-valued antisymmetrized two-electron integrals

$$\langle pq||rs\rangle = \langle rs||pq\rangle^* = \langle rs||pq\rangle \quad (\text{A1})$$

are used. For notational brevity, we use

$$t_{ijab} = \frac{\langle ij||ab\rangle}{\varepsilon_a + \varepsilon_b - \varepsilon_i - \varepsilon_j}, \quad (\text{A2})$$

where ε_p is the energy of the p th orbital in the HF determinant. The f_{pq} denote Fock matrix elements in the canonical MO basis. As before, the subscripts a, b, \dots and i, j, \dots label unoccupied (virtual) and occupied orbitals, respectively, whereas the subscripts p, q, \dots may denote either of them. Furthermore, we use the permutation operator \hat{P}_{pq} which, applied to some expression, permutes the indices p and q therein.

1. IP-ADC(2) matrix vector product

The product of the IP-ADC(2) matrix with a state vector Y is given in terms of the 1h part W_i and the 2h-1p part W_{ija} as

$$W_i = \sum_j I_{ij}^{(1)} Y_j - \frac{1}{\sqrt{2}} \sum_{jkb} \langle jk||bi\rangle Y_{jkb}, \quad (\text{A3})$$

$$W_{ija} = \sum_b f_{ab} Y_{ijb} - (1 - \hat{P}_{ij}) \sum_k f_{ik} Y_{kja} + \frac{1}{\sqrt{2}} \sum_k \langle ij||ka\rangle Y_k, \quad (\text{A4})$$

with

$$I_{ij}^{(1)} = -f_{ij} + \frac{1}{4} (1 + \hat{P}_{ij}) \sum_{abk} t_{ikab} \langle jk||ab\rangle \quad (\text{A5})$$

being the 1h-1h block of the IP-ADC(2) matrix.

2. IP-ADC(3) matrix vector product

The product of the IP-ADC(3) matrix with a state vector Y is given in terms of the 1h part W_i and the 2h-1p part W_{ija} as

$$W_i = \sum_j I_{ij}^{(1)} Y_j + \frac{1}{\sqrt{2}} \sum_{jkb} I_{jkb}^{(2)} Y_{jkb}, \quad (\text{A6})$$

$$W_{ija} = \sum_b f_{ab} Y_{ijb} - (1 - \hat{P}_{ij}) \sum_k f_{ik} Y_{kja} + \frac{1}{2} \sum_{kl} \langle kl||ij\rangle Y_{kla} - (1 - \hat{P}_{ij}) \sum_{lc} \langle la||ic\rangle Y_{lca} + \frac{1}{\sqrt{2}} \sum_k I_{ijka}^{(2)} Y_k, \quad (\text{A7})$$

where $I_{ij}^{(1)}$ is the $1h$ - $1h$ block of the IP-ADC(3) matrix according to

$$I_{ij}^{(1)} = -f_{ij} + \frac{1}{4}(1 + \hat{P}_{ij}) \sum_{abk} t_{ikab} \langle jk || ab \rangle - \frac{1}{8}(1 + \hat{P}_{ij}) \sum_{kcd} t_{jkcd} \times \left[\sum_{ab} t_{ikab} \langle ab || cd \rangle \right] + \frac{1}{2}(1 + \hat{P}_{ij}) \sum_{lac} t_{jlac} \left[\sum_{kb} t_{ikab} \langle kc || lb \rangle \right] - \frac{1}{4}(1 + \hat{P}_{ij}) \sum_{klm} \langle kl || mi \rangle \left[\sum_{ab} t_{klab} t_{mjab} \right] - (1 + \hat{P}_{ij}) \sum_{kac} \langle kc || ia \rangle \times \left[\sum_{lb} t_{klab} t_{jlbc} \right] - \frac{1}{2}(1 + \hat{P}_{ij}) \sum_{kl} \langle ik || jl \rangle \rho_{kl}^{(2)} - (1 + \hat{P}_{ij}) \sum_{ak} \langle ik || ja \rangle \rho_{ka}^{(2)} - \frac{1}{2}(1 + \hat{P}_{ij}) \sum_{ab} \langle ia || jb \rangle \rho_{ab}^{(2)}. \quad (A8)$$

Therein, $\rho_{pq}^{(2)}$ are elements of the second-order correction to the ground state density matrix according to

$$\rho_{ij}^{(2)} = -\frac{1}{2} \sum_{abk} t_{ikab} t_{jkab}, \quad (A9)$$

$$\rho_{ia}^{(2)} = \frac{1}{2(\epsilon_i - \epsilon_a)} \left(\sum_{jbc} t_{ijbc} \langle ja || bc \rangle + \sum_{jkb} t_{jkab} \langle jk || ib \rangle \right), \quad (A10)$$

$$\rho_{ab}^{(2)} = \frac{1}{2} \sum_{ijc} t_{ijac} t_{ijbc}, \quad (A11)$$

and $I_{ijka}^{(2)}$ denotes the $1h$ - $2h$ - $1p$ coupling block of the IP-ADC(3) matrix, which is given as

$$I_{ijka}^{(2)} = \langle ij || ka \rangle - \frac{1}{2} \sum_{cd} t_{ijcd} \langle ka || cd \rangle + (1 - \hat{P}_{ij}) \sum_{cl} t_{ilac} \langle kl || jc \rangle. \quad (A12)$$

3. Pole strength

Given a state vector Y , the relative intensity of the corresponding transition can be calculated as its second-order pole strength,

$$P = x^\dagger x, \quad (A13)$$

where x is the respective spectroscopic amplitude vector. The latter is given in terms of the occupied part x_i and the virtual part x_a as

$$x_i = \sum_j Y_j f_{ji}, \quad (A14)$$

$$x_a = \sum_j Y_j f_{ja} + \sum_{ijb} Y_{ijb} f_{ijba}. \quad (A15)$$

Therein, f_{ij} , f_{ia} , and f_{ijab} denote matrix elements of the so-called effective transition moments, which are given as

$$f_{ij} = \delta_{ij} + \frac{1}{2} \rho_{ij}^{(2)}, \quad (A16)$$

$$f_{ia} = \rho_{ia}^{(2)}, \quad (A17)$$

$$f_{ijab} = -\frac{1}{\sqrt{2}} t_{ijab}, \quad (A18)$$

with $\rho_{ij}^{(2)}$ and $\rho_{ia}^{(2)}$ being elements of the second-order correction to the ground state density matrix as defined by Eqs. (A9) and (A10), respectively.

REFERENCES

- L. S. Cederbaum, W. Domcke, J. Schirmer, and W. von Niessen, "Correlation effects in the ionization of molecules: Breakdown of the molecular orbital picture," *Adv. Chem. Phys.* **65**, 115–159 (1986).
- S. Hüfner, *Photoelectron Spectroscopy—Principles and Applications* (Springer, Berlin, 2003).
- A. Stolow, A. E. Bragg, and D. M. Neumark, *Chem. Rev.* **104**, 1719 (2004).
- G. Wu, P. Hockett, and A. Stolow, *Phys. Chem. Chem. Phys.* **13**, 18447 (2011).
- B. W. D'Andrade, S. Datta, S. R. Forrest, P. Djurovich, E. Polikarpov, and M. E. Thompson, *Org. Electron.* **6**, 11 (2005).
- Electronic Processes in Organic Electronics: Bridging Nanostructure, Electronic States and Device Properties*, Springer Series in Material Science, edited by H. Ishii, K. Kudo, T. Nakayama, and N. Ueno (Springer, Japan, 2015), Vol. 209.
- T. Koopmans, *Physika* **1**, 104 (1933).
- J. F. Janak, *Phys. Rev. B* **18**, 7165 (1978).
- C. Möller and M. S. Plesset, "Note on an approximation treatment for many-electron systems," *Phys. Rev.* **46**, 618 (1934).
- R. J. Bartlett, "Coupled-cluster approach to molecular structure and spectra: A step toward predictive quantum chemistry," *J. Phys. Chem.* **93**, 1697–1708 (1989).
- A. L. Fetter and J. D. Walecka, *Quantum Theory of Many-Particle Systems* (McGraw-Hill, 1971).
- A. A. Abrikosov, L. P. Gorkov, I. E. Dzyaloshinski, and R. A. Silverman, *Methods of Quantum Field Theory in Statistical Physics*, Dover Books on Physics (Dover Publications, 2012).
- J. Simons, "Theoretical studies of negative molecular ions," *Annu. Rev. Phys. Chem.* **28**, 15–45 (1977).
- J. Oddershede, "Polarization propagator calculations," *Adv. Quantum Chem.* **11**, 275–352 (1978).
- M. F. Herman, K. F. Freed, and D. L. Yeager, "Analysis and evaluation of ionization potentials, electron affinities, and excitation energies by the equations of motion-Green's function method," *Adv. Chem. Phys.* **48**, 1–69 (1981).
- Y. Öhrn and G. Born, "Molecular electron propagator theory and calculations," *Adv. Quantum Chem.* **13**, 1–88 (1981).
- L. S. Cederbaum and J. Schirmer, "Green's functions for open-shell atoms and molecules," *Z. Phys.* **271**, 221–227 (1974).
- L. S. Cederbaum and W. Domcke, "Theoretical aspects of ionization potentials and photoelectron spectroscopy: A Green's function approach," *Adv. Chem. Phys.* **36**, 205–344 (1977).
- J. Schirmer, L. S. Cederbaum, and O. Walter, "New approach to the one-particle Green's function for finite fermi systems," *Phys. Rev. A* **28**, 1237–1259 (1983).
- J. Schirmer and G. Angonoa, "On Green's function calculations of the static selfenergy part, the ground state energy and expectation values," *J. Chem. Phys.* **91**, 1754–1761 (1989).
- W. von Niessen, J. Schirmer, and L. S. Cederbaum, "Computational methods for the one-particle Green's function," *Comput. Phys. Rep.* **1**, 57–125 (1984).
- V. G. Zakrzewski and W. von Niessen, "Vectorizable algorithm for Green function and many-body perturbation methods," *J. Comput. Chem.* **14**, 13–18 (1993).
- V. G. Zakrzewski and J. V. Ortiz, "Semidirect algorithms for third-order electron propagator calculations," *Int. J. Quantum Chem.* **53**, 583–590 (1995).
- H. Sekino and R. J. Bartlett, "A linear response, coupled-cluster theory for excitation energy," *Int. J. Quantum Chem.* **26**, 255–265 (1984).
- J. Geertens, M. Rittby, and R. J. Bartlett, "The equation-of-motion coupled-cluster method: Excitation energies of Be and CO," *Chem. Phys. Lett.* **164**, 57–62 (1989).

- ²⁶J. F. Stanton and R. J. Bartlett, "The equation of motion coupled-cluster method. A systematic biorthogonal approach to molecular excitation energies, transition probabilities, and excited state properties," *J. Chem. Phys.* **98**, 7029 (1993).
- ²⁷D. C. Comeau and R. J. Bartlett, "The equation-of-motion coupled-cluster method. Applications to open- and closed-shell reference states," *Chem. Phys. Lett.* **207**, 414–423 (1993).
- ²⁸M. Nooijen and J. G. Snijders, "Coupled cluster approach to the single-particle Green's function," *Int. J. Quantum Chem.* **44**, 55–83 (1992).
- ²⁹J. F. Stanton and J. Gauss, "Analytic energy derivatives for ionized states described by the equation of motion coupled cluster method," *J. Chem. Phys.* **101**, 8938–8944 (1994).
- ³⁰M. Musiał, S. A. Kucharski, and R. J. Bartlett, "Equation-of-motion coupled cluster method with full inclusion of the connected triple excitations for ionized states: IP-EOM-CCSDT," *J. Chem. Phys.* **118**, 1128–1136 (2003).
- ³¹P. U. Manohar, J. F. Stanton, and A. I. Krylov, "Perturbative triples correction for the equation-of-motion coupled-cluster wave functions with single and double substitutions for ionized states: Theory, implementation, and examples," *J. Chem. Phys.* **131**, 114112 (2009).
- ³²O. Walter and J. Schirmer, "The two-particle-hole Tamm-Dancoff approximation (2ph-TDA) for atoms," *J. Phys. B* **14**, 3805–3826 (1981).
- ³³J. Schirmer, A. B. Trofimov, and G. Stelter, "A non-Dyson third-order approximation scheme for the electron propagator," *J. Chem. Phys.* **109**, 4734–4744 (1998).
- ³⁴A. B. Trofimov and J. Schirmer, "Molecular ionization energies and ground- and ionic-state properties using a non-Dyson electron propagator approach," *J. Chem. Phys.* **123**, 144115 (2005).
- ³⁵M. Schneider, D. Y. Soshnikov, D. M. P. Holland, I. Powis, E. Antonsson, M. Patanen, C. Nicolas, C. Miron, M. Wormit, A. Dreuw, and A. B. Trofimov, "A fresh look at the photoelectron spectrum of bromobenzene: A third-order non-Dyson electron propagator study," *J. Chem. Phys.* **143**, 144103 (2015).
- ³⁶F. Mertins and J. Schirmer, "Algebraic propagator approaches and intermediate-state representations. I. The biorthogonal and unitary coupled-cluster methods," *Phys. Rev. A* **53**, 2140–2152 (1996).
- ³⁷F. Mertins, J. Schirmer, and A. Tarantelli, "Algebraic propagator approaches and intermediate-state representations. II. The equation-of-motion methods for $N, N \pm 1$, and $N \pm 2$ electrons," *Phys. Rev. A* **53**, 2153–2168 (1996).
- ³⁸J. Schirmer and F. Mertins, "Size consistency of an algebraic propagator approach," *Int. J. Quantum Chem.* **58**, 329 (1996).
- ³⁹J. Schirmer and F. Mertins, "Review of biorthogonal coupled cluster representations for electronic excitation," *Theor. Chem. Acc.* **125**, 145–172 (2010).
- ⁴⁰M. Wormit, D. R. Rehn, P. H. P. Harbach, J. Wenzel, C. M. Krauter, E. Epifanovsky, and A. Dreuw, "Investigating excited electronic states using the algebraic diagrammatic construction (ADC) approach of the polarisation propagator," *Mol. Phys.* **112**, 774–784 (2014).
- ⁴¹Y. Shao, Z. Gan, E. Epifanovsky, A. T. B. Gilbert, M. Wormit, J. Kussmann, A. W. Lange, A. Behn, J. Deng, X. Feng, D. Ghosh, M. Goldey, P. R. Horn, L. D. Jacobson, I. Kaliman, R. Z. Khaliullin, T. Kuš, A. Landau, J. Liu, E. I. Proynov, Y. M. Rhee, R. M. Richard, M. A. Rohrdanz, R. P. Steele, E. J. Sundstrom, H. L. Woodcock, P. M. Zimmerman, D. Zuev, B. Albrecht, E. Alguire, B. Austin, G. J. O. Beran, Y. A. Bernard, E. Berquist, K. Brandhorst, K. B. Bravaya, S. T. Brown, D. Casanova, C.-M. Chang, Y. Chen, S. H. Chien, K. D. Closser, D. L. Crittenden, M. Diedenhofen, R. A. DiStasio, H. Do, A. D. Dutoi, R. G. Edgar, S. Fatehi, L. Fusti-Molnar, A. Ghysels, A. Golubeva-Zadorozhnaya, J. Gomes, M. W. D. Hanson-Heine, P. H. P. Harbach, A. W. Hauser, E. G. Hohenstein, Z. C. Holden, T.-C. Jagau, H. Ji, B. Kaduk, K. Khistyayev, J. Kim, J. Kim, R. A. King, P. Klunzinger, D. Kosenkov, T. Kowalczyk, C. M. Krauter, K. U. Lao, A. D. Laurent, K. V. Lawler, S. V. Levchenko, C. Y. Lin, F. Liu, E. Livshits, R. C. Lochan, A. Luenser, P. Manohar, S. F. Manzer, S.-P. Mao, N. Mardirossian, A. V. Marenich, S. A. Maurer, N. J. Mayhall, E. Neuscamman, C. M. Oana, R. Olivares-Amaya, D. P. O'Neill, J. A. Parkhill, T. M. Perrine, R. Peverati, A. Prociuk, D. R. Rehn, E. Rosta, N. J. Russ, S. M. Sharada, S. Sharma, D. W. Small, A. Sodt, T. Stein, D. Stück, Y.-C. Su, A. J. W. Thom, T. Tsuchimochi, V. Vanovschi, L. Vogt, O. Vydrov, T. Wang, M. A. Watson, J. Wenzel, A. White, C. F. Williams, J. Yang, S. Yeganeh, S. R. Yost, Z.-Q. You, I. Y. Zhang, X. Zhang, Y. Zhao, B. R. Brooks, G. K. L. Chan, D. M. Chipman, C. J. Cramer, W. A. Goddard, M. S. Gordon, W. J. Hehre, A. Klamt, H. F. Schaefer, M. W. Schmidt, C. D. Sherrill, D. G. Truhlar, A. Warshel, X. Xu, A. Aspuru-Guzik, R. Baer, A. T. Bell, N. A. Besley, J.-D. Chai, A. Dreuw, B. D. Dunietz, T. R. Furlani, S. R. Gwaltney, C.-P. Hsu, Y. Jung, J. Kong, D. S. Lambrecht, W. Liang, C. Ochsenfeld, V. A. Rassolov, L. V. Slipchenko, J. E. Subotnik, T. Van Voorhis, J. M. Herbert, A. I. Krylov, P. M. W. Gill, and M. Head-Gordon, "Advances in molecular quantum chemistry contained in the Q-Chem 4 program package," *Mol. Phys.* **113**, 184–215 (2015).
- ⁴²E. Epifanovsky, M. Wormit, T. Kuš, A. Landau, D. Zuev, K. Khistyayev, P. Manohar, I. Kaliman, A. Dreuw, and A. I. Krylov, "New implementation of high-level correlated methods using a general block tensor library for high-performance electronic structure calculations," *J. Comput. Chem.* **34**, 2293–2309 (2013).
- ⁴³E. R. Davidson, "The iterative calculation of a few of the lowest eigenvalues and corresponding eigenvectors of large real-symmetric matrices," *J. Comput. Phys.* **17**, 87–94 (1975).
- ⁴⁴T. H. Dunning, "Gaussian basis sets for use in correlated molecular calculations. I. The atoms boron through neon and hydrogen," *J. Chem. Phys.* **90**, 1007–1023 (1989).
- ⁴⁵D. E. Woon and T. H. Dunning, "Gaussian basis sets for use in correlated molecular calculations. V. Core-valence basis sets for boron through neon," *J. Chem. Phys.* **103**, 4572–4585 (1995).
- ⁴⁶K. A. Peterson and T. H. Dunning, "Accurate correlation consistent basis sets for molecular core-valence correlation effects: The second row atoms Al–Ar, and the first row atoms B–Ne revisited," *J. Chem. Phys.* **117**, 10548–10560 (2002).
- ⁴⁷D. M. Close, "Calculated vertical ionization energies of the common α -amino acids in the gas phase and in solution," *J. Phys. Chem. A* **115**, 2900–2912 (2011).
- ⁴⁸I. Ljubić, A. Kivimäki, M. Coreno, S. Kazazić, and I. Novak, "Characterisation of the electronic structure of galvinoxyl free radical by variable energy UPS, XPS and NEXAFS spectroscopy," *Phys. Chem. Chem. Phys.* **20**, 2480–2491 (2018).
- ⁴⁹P. H. Cannington and N. S. Ham, "He(I) and He(II) photoelectron spectra of glycine and related molecules," *J. Electron Spectrosc. Relat. Phenom.* **32**, 139–151 (1983).
- ⁵⁰A. Kramida, Y. Ralchenko, J. Reader, and NIST ASD Team, NIST Atomic Spectra Database (ver. 5.5.2), [Online]. Available: <https://physics.nist.gov/asd> [2018 January 17], National Institute of Standards and Technology, Gaithersburg, MD, 2018.
- ⁵¹B. N. Plakhutin, "Koopmans' theorem in the Hartree-Fock method. General formulation," *J. Chem. Phys.* **148**, 094101 (2018).
- ⁵²R. T. Wiedmann, R. G. Tonkyn, M. G. White, K. Wang, and V. McKoy, "Rotationally resolved threshold photoelectron spectra of OH and OD," *J. Chem. Phys.* **97**, 768–772 (1992).
- ⁵³J. M. Dyke, N. Jonathan, A. Morris, A. Ridha, and M. J. Winter, "Vacuum ultraviolet photoelectron spectroscopy of transient species. XVII. The $\text{SiH}_3(\text{X}^2\text{A}_1)$ radical," *Chem. Phys.* **81**, 481–488 (1983).
- ⁵⁴J. Dyke, N. Jonathan, E. Lee, and A. Morris, "Vacuum ultraviolet photoelectron spectroscopy of transient species. Part 7.—The methyl radical," *J. Chem. Soc., Faraday Trans. 2* **72**, 1385–1396 (1976).
- ⁵⁵J. M. Dyke, A. R. Ellis, N. Keddar, and A. Morris, "A reinvestigation of the first band in the photoelectron spectrum of the ethyl radical," *J. Phys. Chem.* **88**, 2565–2569 (1984).
- ⁵⁶T. Koenig, W. Snell, and J. C. Chang, "The He(I) photoelectron spectra of benzyl and α -cyanoisopropyl radicals," *Tetrahedron Lett.* **17**, 4569–4572 (1976).
- ⁵⁷J. K. Kochi, *Free Radicals* (Wiley, New York, 1973).
- ⁵⁸I. Shibata, K. Nakamura, A. Baba, and H. Matsuda, *Tetrahedron Lett.* **31**, 6381 (1990).
- ⁵⁹C. Thom, P. Kociński, and K. Jarowicki, *Synthesis* **1993**, 475.